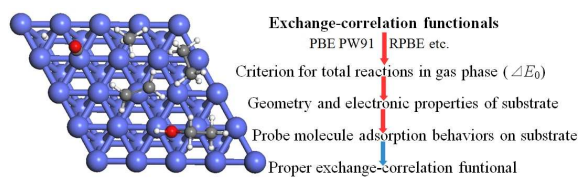# PCCP

Accepted Manuscript

This is an *Accepted Manuscript*, which has been through the Royal Society of Chemistry peer review process and has been accepted for publication.

Accepted Manuscripts are published online shortly after acceptance, before technical editing, formatting and proof reading. Using this free service, authors can make their results available to the community, in citable form, before we publish the edited article. We will replace this *Accepted Manuscript* with the edited and formatted *Advance Article* as soon as it is available.

You can find more information about *Accepted Manuscripts* in the **Information for Authors**.

A step-by-step approach for screening a reliable exchange-correlation functional in the computational catalysis on surface is proposed.

Physical Chemistry & Chemical Physics

ARTICLE TYPE

Choosing a proper exchange-correlation functional for the computational catalysis on surface

Bo-Tao Teng,*[a,b] Xiao-Dong Wen,[c] Maohong Fan,*[b] Feng-Min Wu,[a] Yulong Zhang[d]

To choose a proper functional among the diverse density functional approximations of the electronic exchange-correlation energy for a given system is the basis for obtaining accurate results of theoretical calculations. In this work, we firstly propose an approach by comparing the calculated $\triangle E_0$ with the theoretical reference data based on the corresponding experimental results in gas phase reaction. With $\triangle E_0$ being a criterion, three most typical and popular

10 exchange-correlation functionals (PW91, PBE and RPBE) were systematically compared in terms of the typical Fischer-Tropsch synthesis reactions in gas phase. In addition, the verifications of geometrical and electronic properties of modeling catalysts, as well as the adsorption behaviors of typical probe molecule on modeling catalysts are also suggested for further screening proper functionals. After systematical comparison of CO adsorption behaviors on Co(0001) calculated by PW91, PBE, and RPBE, RPBE functional is better than the other two in view of FTS reactions in gas phase and CO adsorption

15 behaviors on cobalt surface. The present work shows general implications for how to choose a reliable exchange-correlation functional in the computational catalysis on surface.

[a] College of Chemistry and Life Sciences, Zhejiang Normal University, Jinhua 321004, China;
[b] Department of Chemical & Petroleum Engineering, University of Wyoming, Laramie, WY 82071, USA
[c] Theoretical Division, Los Alamos National Laboratory, Los Alamos, NM 87545, USA;
[d] Western Research Institute, Laramie, WY 82070, USA
Corresponding authors. Email: tbt@zjnu.cn; mfan@uwyo.edu

1. INTRODUCTION

With the rapid development of computing capacity, as well as new theoretical methods and tools with high efficiency, theoretical simulation and design of catalysts has been extensively performing.[1-6] Human beings are gradually realizing the dream into reality, in which designs and simulates heterogeneous catalysts at an atomic and molecular level.[7-13] Although systematically theoretical investigations of the structure and properties of catalysts, as well as their catalytic performances, greatly enhance our understanding of the catalytic process, the accurate and authentic theoretical results greatly depend on the reasonable choice of electronic exchange-correlation functional.[14] Therefore, how to choose a proper functional among the diverse density functional approximations of the electronic exchange-correlation energy for a modeling catalyst under consideration is the key before the further theoretical calculation.

The general way to check the rationality of an exchange-correlation functional for the concerned catalytic system, is to compare the calculated structural parameters and electronic properties of modeling catalysts with the experimental data available current,[15-16] or the theoretical values reported in the literatures. However, one might obtain various results from different exchange-correlation functionals.[17-18] On the other hand, some key experimental data to verify the reliability of the theoretical methods, such as reactant and product adsorption energies and geometrical parameters, especially the activation energy barriers of elementary reactions on catalyst surface, etc., are generally scarce due to the complexity of heterogeneous catalysis, as well as the material and pressure gaps between the practical and theoretical modeling catalysts.[19]

Compared with the shortage of precise experimental data for heterogeneous catalysis, there is a systematic database of the thermodynamics and other properties for substances and reactions in gas phase, which has been accumulated for centuries.[20] How to use the existing accurate database of reactions in gas phase to provide important information for theoretical catalysis, especially for choosing a reasonable electronic exchange-correlation functional, is a challenge for theoretical research.

Very recently, using Fischer-Tropsch synthesis (FTS) as a probe reaction, Zhang and Xu [14] purposed a talented approach to characterize the reliability of different exchange-correlation functionals for FTS reaction based on a Born–Haber cycle. The chain initiations, growth, terminations, as well as the total reaction enthalpy changes calculated by different electronic exchange-correlation functionals (B3LYP, PBE and XYG3) were systematically compared. Their important contribution for heterogeneous catalysis pointed out that the theoretical results on surfaces would be less meaningful if gas-phase behavior cannot first be suitably determined. Therefore, the elementary reaction steps in gas phase should be firstly tested and verified for the theoretical methods. However, the corresponding testification is generally omitted for the

enthalpies of free molecules could not be directly obtained by most of theoretical packages. The immediate results of the total electronic energy and the corresponding differences (ΔE_0) in gas phase reaction are quite different from the enthalpy and ΔH values. Meanwhile, there are not the corresponding experimental data of ΔE_0 to verify their validity.

In this work, we propose an approach how to test the reliability of different electronic exchange-correlation functionals by comparing the calculated ΔE_0 with the theoretical reference data based on the corresponding experimental results in gas phase reaction. In addition, to further characterize the reliability of different exchange-correlation functionals, the verifications of geometrical and electronic properties of modeling catalysts, as well as the adsorption behaviors of typical probe molecule on modeling catalysts are also proposed. These confirmations will be helpful to obtain a reliable exchange-correlation functional for heterogeneous catalytic system under consideration.

2. COMPUTATIONAL DETAILS

It was reported by Zhang and Xu[14] that the calculated heats of the Fischer Tropsch reactions to form alkane, alkene, and alkanol in gas phase at the B3LYP/6-311+G(d,p) level by Gaussian is well consistent with those of experimental values. Therefore, the geometry of CO, H_2, H_2O, as well as alkanes, alkenes, and alcohols (C1-C3) in gas phase were firstly optimized at the B3LYP/6-311+G(d,p) level by Gaussian03 package,[21] by which the corresponding electronic energy at 0 K were obtained. Then, the analytical harmonic frequency was calculated at the same level to ensure that the geometrical structures are the local minimum without imaginary frequencies. Simultaneously, the thermal enthalpies of reactants and products at 298.15 K were obtained by calculating the zero-point energy (ZPE) and thermo-corrections. Correspondingly, the electronic energy differences at 0 K and the reaction enthalpies of FTS reactions in gas phase at 298.15 K and 1 atm were calculated as follows:

$$\Delta E = E_{\text{product}} - nE_{\text{CO}} - mE_{H_2}$$

$$\Delta H = H_{\text{product}} - nH_{\text{CO}} - mH_{H_2}$$

where product represents alkanes, alkenes, alcohols (C1-C3), as well as water formed during reaction; n and m mean the molecular number of CO and H_2 in FTS reaction.

The electronic energy differences of FTS reactions in gas phase were also calculated by Vienna *ab initio* simulation package (VASP) code,[22] which bases on the plane-wave periodical density functional theory. Using the generalized gradient approximation (GGA) method,[23] three most typical and popular electronic exchange-correlation functions (PW91,[24] PBE,[25] and RPBE[17]) were calculated in turn. The cores were represented by the projector augmented wave (PAW) potentials.[26] The Kohn-Sham one-electron wave functions were expanded in a plane-wave basis with a cutoff energy of 400 eV. The Brillouin-zone integration was approximated by a sum over special k-

points chosen using the Monkhorst-Pack(MP) grids.[27] A Gaussian smearing method was used for the optimization of free molecules in gas phase reaction; while a Methfessei-Paxton smearing method for metallic system,
5 Co lattice optimization and CO adsorption on Co(0001) surface. The corresponding smearing width was set to 0.1 eV. The Kohn-Sham equations were solved self-consistently, and the convergence criteria for the energy calculation was set to 1.0×10^{-4} eV; while the maximum
10 Hellmann-Feynman force tolerance of structure optimization was set to 0.03 eV/Å.

For the optimization of free molecules, a molecule was put into a $15 \times 15 \times 15 Å^3$ cube and was fully relaxed with the k point of $1 \times 1 \times 1$. For CO adsorption upon
15 Co(0001) surface, a p(2×2) R60^o superlattice with four-layer cobalt atoms was used in the present work, in which the top two layer atoms were fully relaxed. The corresponding k point was set to $5 \times 5 \times 1$. According to the test of cutoff energy, smearing width and k point listed in
20 Table S1 of supplementary materials, the corresponding sets are converged. To eliminate the interactions between vertical slabs, the vacuum height was set as 12 Å.[28] For verification of the one-side model, a periodical two-side model with seven-layer Co atoms was also tested. Based
25 on the adsorption parameters listed in Table S2 and configurations shown in Fig. S1 of supplementary material, the adsorption energy differences predicted by the two models are less than 0.02 eV, and the C-O bond length differences are less than 0.002 Å. Therefore, the model
30 used herein is reliable.

Molecular CO adsorption at the different sites of Co(0001) was systematically studied, and the corresponding adsorption energy was defined as:

$$E_{ads} = E_{CO/substrat} - [E_{CO} + E_{substrate}]$$

35 where $E_{CO/substrate}$ is the total energy of the substrate with adsorbed CO; E_{CO} and $E_{substrate}$ are the energies of free molecular CO and an isolated substrate, respectively. Therefore, a negative value means exothermic adsorption, while a positive one means endothermic adsorption. The
40 more negative the adsorption energy, the stronger the adsorption.

3. RESULTS AND DISCUSSION

3.1 Reliability of the $\triangle E_0$ standard

The immediate output by most of theoretical packages
45 is the total electronic energy (E_{elec}) at 0 K. To calculate the enthalpy of a free molecule at the specified temperature and pressure, frequency analysis must be carried out to give the zero-point vibrational energy (ZPVE). Furthermore, the effects of molecular translation, rotation
50 and vibration, as well as the volumetric work must be involved in the calculation. That is, the enthalpy of a specified molecule in gas phase is equal to the sum of E_{elec}, ZPE, E_{trans}, E_{rot}, E_{vib}, as well as PV. Correspondingly, the $\triangle H$ for a reaction of A+B=AB can be calculated according
55 to Eq. 1.

$$\triangle H = H_{AB} - H_A - H_B \qquad \text{(Eq. 1)}$$

For most of theoretical packages based on the

periodical density functional theory, such as Vienna *ab initio* simulation package (VASP), Cambridge Sequential
60 Total Energy Package (CASTEP),[29-30] etc., the enthalpy will be obtained by calculating the phonon frequencies with linear response on the basis of the density functional perturbation theory.[31-32]

Could we use the $\triangle E_0$ as a standard to verify the
65 reliability of exchange-correlation functionals in gas phase reaction? On the basis of thermodynamic principles, the volumetric work, E_{trans}, E_{rot}, and E_{vib} of a specified molecule at the specified temperature and pressure are constants. Therefore, the enthalpy value is mainly
70 determined by its E_{elec} and ZPE. As we known, the zero-point energy and total electronic energy are both dependent on the optimized geometry and exchange-correlation functional. Therefore, a reliable exchange correlation functional must lead to the reasonable structure and
75 accurate E_{elec} value of a molecule. Correspondingly, it will obtain an accurate $\triangle E_0$ value, as calculated by Eq. 2, for a reaction of A+B=AB in gas phase reaction. In turn, $\triangle E_0$ can be used as one of the most important standards to estimate the reliability of exchange correlation functional.

80 $$\triangle E_0 = E_{elec,AB} - E_{elec,A} - E_{elec,B} \qquad \text{(Eq. 2)}$$

According to the analysis above, if a theoretical $\triangle H_{cal}$ of a specified reaction in gas phase is well consistent with the experimental value, the corresponding theoretical $\triangle E_0$ must be reliable, and then can be used as a
85 standard to estimate the reliability of exchange-correlation functional.

It was reported by Zhang and Xu [14] that the calculated enthalpy changes of the elementary steps of Fischer Tropsch reactions, chain initiation, growth, termination, as
90 well as the total reaction to form alkane, alkene, and alkanol in gas phase at the B3LYP/6-311+G(d,p) level by Gaussian are well consistent with those of experimental values. Therefore, the corresponding theoretical $\triangle E_0$ can be used as a reference value to test the reliability of
95 different electronic exchange-correlation functions in other solid simulation packages. The following section will show how to use the referred $\triangle E_0$ to screen a proper exchange-correlation functional in heterogeneous catalyst.

3.2 Verification of $\triangle E_0$ values of FTS reactions in
100 gas phase

Fischer-Tropsch synthesis which converts syngas into liquid fuels and chemicals has been paid much attention these years due to the depleting resources of crude oil all over the world.[33-35] A theoretical study of FTS reaction
105 behaviors on Fe or Co-based catalysts is of great importance for developing industrial catalysts with high performance.[36] Therefore, the electronic energy changes of the typical alkanes, alkenes, and alcohols in gas phase FTS reactions are calculated to screen the possibly reliable
110 exchange-correlation functionals herein.

The $\triangle H_{cal}$ of the typical FTS reactions to form alkane, alkene, and alkanol in gas phase at 298.15 K and atmospheric pressure, as well as $\triangle E_0$ are calculated at the

level of B3LYP/6-311+G(d,p) by using Gaussian 03 Package, as listed in Table 1. One can learn from Table 1 that the calculated $\triangle H_{cal}$ values are well consistent with the experimental ones, as well as the values reported by Zhang and Xu.[14] Therefore, the corresponding $\triangle E_0$ calculated at the B3LYP/6-311+G(d,p) level for the typical FTS reactions in gas phase can be used as the referred values to verify the reliability of different electronic exchange-correlation functionals. For further verification, the $\triangle H_{cal}$ values calculated by cc-pVTZ basis sets [37] which is directly comparable to the plane-wave quality, as well as by phonon calculation [38] using the finite-different approach by VASP code, are listed in Table S3 of

supplementary material. It can be learned from Table S3 that the $\triangle H_{cal}$ values calculated by the latter two methods are very close to ones by B3LYP/6-311+G(d,p). This further supports the reliability of $\triangle E_0$ standard for screening a proper exchange-correlation functional in computational catalysis. It can be also learned from Table 1 that the $\triangle E_0$ values are generally less than $\triangle H_{cal}$ at 298.15 K and atmospheric pressure for the latter one includes the ZPE energy, molecular translation, rotation and vibration, as well as volumetric work, which leads to the increase of total energy for given system.

Table 1 Enthalpy and electronic energy changes (eV) of alkane, alkene and alkanol formation reactions

	$\triangle H_{cal}$ B3LYP	$\triangle H_{exp}$	$\triangle E_{0,ref}$ B3LYP	$\triangle E_0$					
				PW91	Error %	PBE	Error %	RPBE	Error %
CH_4	-2.17	-2.14	-2.85	-3.19	-11.94	-3.17	-11.38	-2.80	1.74
C_2H_6	-3.60	-3.59	-4.83	-5.45	-12.83	-5.42	-12.24	-4.66	3.55
C_3H_8	-5.10	-5.16	-6.86	-8.00	-16.52	-7.96	-15.93	-6.79	1.11
C_6H_{14}	-9.58	-9.90	-12.95	-15.30	-18.14	-15.22	-17.54	-12.83	0.95
$C_{10}H_{22}$	-15.56	-16.19	-21.07	-25.01	-18.70	-24.88	-18.11	-20.85	1.02
C_2H_4	-2.21	-2.18	-3.16	-3.80	-20.27	-3.77	-19.36	-3.15	0.04
C_3H_6	-3.87	-3.87	-5.34	-6.40	-19.85	-6.36	-19.13	-5.34	0.00
C_6H_{12}	-8.35	-8.60	-11.43	-13.66	-19.53	-13.58	-18.86	-11.33	0.82
$C_{10}H_{20}$	-14.33	-14.90	-19.54	-23.33	-19.38	-23.20	-18.69	-19.31	1.20
CH_3OH	-0.99	-0.94	-1.54	-1.92	-24.21	-1.90	-22.91	-1.52	1.40
C_2H_5OH	-2.65	-2.65	-3.73	-4.50	-20.63	-4.46	-19.75	-3.68	1.29
C_3H_7OH	-4.14	-4.40	-5.76	-6.93	-20.45	-6.88	-19.49	-5.69	1.20
$C_6H_{13}OH$	-8.62	-8.93	-11.84	-14.22	-20.05	-14.13	-19.34	-11.72	1.04
$C_{10}H_{21}OH$	-14.60	-15.11	-19.96	-23.96	-20.03	-23.81	-19.31	-19.76	1.00

As listed in Table 1, the $\triangle E_0$ values calculated by PW91 and PBE functionals are much similar since the PBE functional is developed to mimic the PW91 functional, but with fewer parameters and a simpler functional form.[25] It was reported by Hammer et al.[17] that the two methods have very similar gradient-dependent exchange correlation energy contributions, $E_{chem,GGA} - E_{chem,LDA} = \int_A \Delta E_{chem,GGA}(r)\,dx\,dy$, which correspondingly yields almost identical numerical $\triangle E_0$ values.

Simultaneously, one can learn from Table 1 that the $\triangle E_0$ value calculated by RPBE functional is very close to their corresponding references. This might be attributed to its revised form of $F_X(s)$, the local exchange enhancement factor, $F_X(s) = 1 + k - \dfrac{k}{1 + \mu s^2/k}$ in PBE is substituted for $F_X(s) = 1 + k(1 - e^{-\mu s^2/k})$ in RPBE. The modification of $F_X(s)$ in PBE functional greatly improves the chemical energies without violating the local Leib-Oxford bound. Correspondingly, the $\triangle E_0$ values calculated by RPBE functional are more accurate than those by PBE and PW91 ones. Therefore, RPBE is better than the other two

functionals in terms of the reaction energy changes in gas phase.

3.3 Verification of geometrical and magnetic properties of modeling catalyst

In addition to the accurate prediction of the $\triangle E_0$ values for a given reaction in gas phase, the functional should be also tested for the modeling catalyst, typically including its geometrical parameters, electronic or magnetic properties. The theoretical and experimental comparison of adsorption behaviors of probe molecules on a given system would be helpful to choose a reasonable functional if the experimental data in surface science at ultra high vacuum conditions are available.

Here, the adsorption behaviors of CO probe molecule on Co(0001) are chosen as a demonstration. The lattice parameters and magnetic moment of the hexagonal close-packed cobalt are systematically calculated and listed in Table 2. Similar to the $\triangle E_0$ calculation, the lattice parameters of a, c and c/a ratio, as well as the magnetic moment calculated by PW91 are also the same as those of PBE, which further support the similar results obtained by PW91 and PBE.[25] Furthermore, the a and c values calculated by PW91 and PBE are shorter than their experimental data, indicating that the two functionals

might predict more delocalization character for d electrons. The computed value of a (2.516 Å) by RPBE is slightly longer than the experiment (2.507 Å). RPBE give a good prediction on c, 4.069 Å, the same as the experimental one. The magnetic moments of Co calculated by the three exchange-correlation functionals are all in good agreement with the experimental data. In summary, RPBE functional is better than the other two although there are not significant differences in bulk geometry and magnetic moments of cobalt.

Table 2 Lattice parameters and magnetic moment of Co

	PW91	PBE	RPBE	exp
a / Å	2.49	2.50	2.52	2.51
c / Å	4.02	4.03	4.07	4.07
c/a	1.61	1.62	1.62	1.62
V / Å^3	21.68	21.72	22.31	22.15
Magnetic moment / μB	3.20	3.22	3.25	3.16

3.4 Verification of adsorption behaviors of probe molecule on modeling catalyst

Before a systematical investigation of adsorption behaviors and reaction mechanism for a given system, it is necessary to do a preliminary test of probe molecule adsorption behaviors on the modeling catalyst to select a rational functional. CO adsorption behaviors at the different sites on Co(0001) are systematically calculated by PW91, PBE, and RPBE functionals. The corresponding adsorption energies and geometrical parameters are listed in Table 3 and 4, respectively.

Table 3 CO adsorption energies (E_{ads} / eV) on Co(0001) at 0.25 ML coverage

	PW91	PBE	RPBE	exp[39]
top	-1.70	-1.67	-1.37	-1.33
fcc	-1.70	-1.68	-1.27	
hcp	-1.71	-1.68	-1.27	
bridge	-1.65	-1.62	-1.23	

One can see from Table 3 that the adsorption energies of CO calculated by PW91 and PBE functionals at the top, bridge, fcc and hcp hollow sites on Co(0001) are very similar, which are also well consistent the theoretical values reported by Gajdoš et al.[18] The most stable configurations optimized by the two functionals are both at the hcp site, which disagrees with the experimental observation that the most stable configuration locates at the top site when the CO coverage is less than 0.33 ML.[40] Furthermore, the adsorption energies at top site predicated by PW91 (-1.70 eV) and PBE (-1.67 eV) functionals are also stronger than the experimental one, -1.33 eV at 0.25 ML coverage.[39]

However, the most stable structure of CO on Co(0001) calculated by RPBE functional is located at the top site with an adsorption energy of -1.37 eV, which is well in agreement with the experimental results.[39, 41] Different from the significant differences in adsorption energies predicted by the three functionals, there are no obvious distinctions in geometrical structures according to the comparison of the bond lengths of C-O and Co-C listed in Table 4.

Table 4 Geometric structures (Å) of CO adsorbed on Co(0001)

		PW91	PBE	RPBE	exp[41]
d$_{C-O}$	Free CO	1.142	1.144	1.148	1.143
	top	1.167	1.168	1.173	1.17±0.06
d$_{C-O}$	fcc	1.192	1.193	1.199	
	hcp	1.194	1.196	1.201	
	bridge	1.187	1.189	1.194	
	top	1.752	1.749	1.764	1.78±0.06
		1.984	1.975	1.993	
	fcc	1.984	1.991	2.002	
		1.984	1.998	2.008	
d$_{Co-C}$		1.972	1.971	1.989	
	hcp	1.976	1.976	1.987	
		1.991	1.991	1.999	
	bridge	1.900	1.903	1.922	
		1.925	1.930	1.930	

To obtain the energy contribution upon CO adsorption on Co(0001), the deformation energies contributed by CO and slab for different configurations are also calculated using PW91, PBE and RPBE functionals, and were listed in Table 5. E_{def} is defined as Eq. 3.

$$E_{def}=E_a-E_b \qquad (Eq. 3)$$

where E_a is the energy of deformed CO or slab upon adsorption; while E_b is the energy of optimized free CO or bare slab.

According to the data listed in Table 5, the deformation energies of CO and slab calculated by different functionals are almost the same.

Table 5 Deformation energies contributed by CO and slab

	top	fcc	hcp	bridge
E_{def} for CO				
PW91	0.03	0.12	0.13	0.10
PBE	0.03	0.13	0.14	0.11
RPBE	0.04	0.13	0.14	0.11
E_{def} for slab				
PW91	0.03	0.03	0.03	0.02
PBE	0.03	0.03	0.03	0.02
RPBE	0.03	0.04	0.03	0.02

For further verification, Table 6 listed the calculated frequencies and the corresponding frequency shifts of free CO and CO adsorbed on Co(0001) by PW91, PBE, and RPBE. According to Table 6, the calculated stretch frequencies of free CO are all slightly less than the experimental value, 2143 cm^{-1}. The lowest one is 2107 cm^{-1} by RPBE functional. Similar results are also observed for CO adsorbed at different sites of Co(0001). However, the relative error of the calculated CO frequency at the top site on Co(0001) by RPBE is less than 2.5 % compared with the experimental value, and less than 1 % compared with the theoretical data by PW91 and PBE functionals. Furthermore, the frequency shifts of CO at the top site of Co(0001) calculated by PBE and RPBE functionals are

very close to the experimental one, 143 cm^{-1}.

Table 6 Frequencies (cm^{-1}) of CO on Co(0001) and corresponding shifts (cm^{-1}) compared to free CO

	PW91		PBE		RPBE		exp[42]
	Freq.	Shift	Freq.	Shift	Freq.	Shift	
Free CO	2136		2125		2107		2143
top	1972	164	1972	153	1953	154	2000
fcc	1779	357	1778	347	1752	355	
hcp	1763	373	1760	365	1739	368	
bridge	1812	324	1811	314	1788	319	

The CO adsorption behaviors on Co(0001) are also calculated by Grimme DFT-D scheme using PBE and RPBE functionals.[43-44] The corresponding adsorption energies are listed in Table 7. It is very interesting to find that the most stable configurations calculated by PBE and RPBE functionals using DFT-D are the same as standard DFT method, indicating that the van der Waals correction does not affect the adsorption configurations. On the other hand, the adsorption energies calculated by DFT-D method are lower than those by stand DFT about 0.32-0.36 eV. Important, the trend of adsorption energy from van der Waals correction is still same to the one without van der Waals correction. We also calculate the interaction energy between the adsorbed CO without substrate by DFT-D scheme. It is generally less than 0.05 eV. Exploring the possible electronic nature of the increase in adsorption energy of CO on Co(0001) by DFT-D method is very interesting and will be further investigated in our future work.

Table 7 E_{ads} by DFT-D and $\triangle E_{ads}$ (eV) compared to standard DFT on Co(0001) at 0.25 ML

	E_{ads} (PBE)	$\triangle E_{ads}$ (PBE)	E_{ads} (RPBE)	$\triangle E_{ads}$ (RPBE)
top	-2.01	0.34	-1.69	0.32
fcc	-2.04	0.36	-1.62	0.35
hcp	-2.04	0.36	-1.62	0.34
bridge	-1.97	0.35	-1.57	0.33

Therefore, the RPBE functional is better than the other two in terms of the adsorption behaviors on Co(0001), especially in the accurate description of the most stable adsorption site and adsorption energy.

3.5 Electronic properties

To shed light upon the electronic interactions between CO and Co(0001), the partial density of states (PDOS) for CO adsorbed at different sites and surface cobalt atoms calculated by RPBE functional are shown in Fig. 1. Compared with free CO, the peaks of the highest occupied molecular orbital (HOMO, 5σ) for adsorbed CO shift downwards in energy about 6 eV and overlap with 1π orbital, as shown in Fig. 1(b)-(e). This indicates that strong chemical interactions occur upon CO adsorption, which is well consistent with the high adsorption energies. Furthermore, a low and broad peak in the range of -0.5~-

1.5 eV appears, which corresponds to the lowest unoccupied molecular orbital (LUMO, 2π*) of adsorbed CO. It implies that the electrons of Co(0001) feedbacks to the 2π* of CO, which also supports the strong electronic interactions between CO and Co(0001). As shown in Fig. 1(f), the peak of d orbitals for surface Co atoms slightly shifts downwards and the corresponding peak area near Fermi energy level also slightly reduces compared to that of bare surface when CO adsorbs at Co(0001). This result further verifies the electronic backdonation to the 2π* orbital of CO.
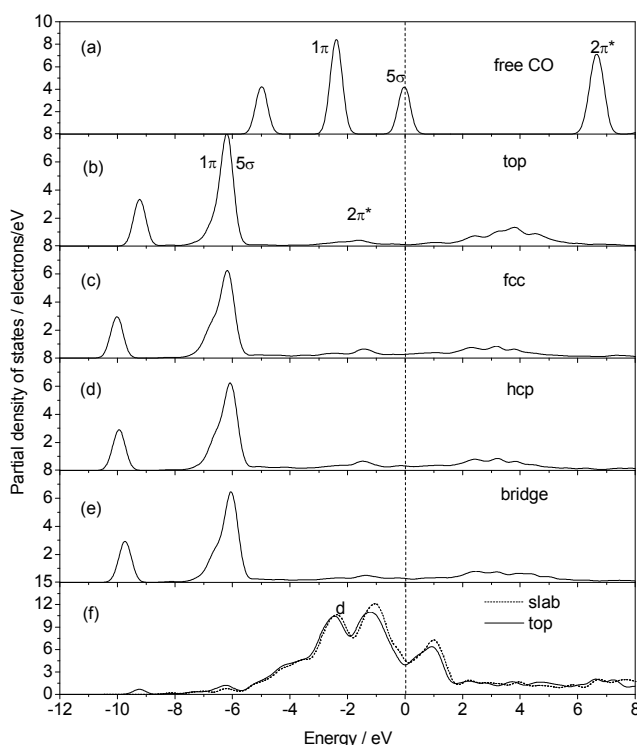

Fig. 1. Partial density of states (PDOS) of CO(a) and Co atoms. (a): free CO; (b)-(e) CO at the top, fcc, hcp and bridge sites on Co(0001); (f) solid line for Co atoms with CO adsorbed at the top site on Co(0001); the dot line for Co atoms at clean surface. The vertical dashed line indicates the Fermi level at 0 eV.

To give a further insight into the electronic nature of interactions upon CO adsorption on Co(0001), the magnetic moments and corresponding changes of surface Co atoms are listed in Table 8. According to the data in Table 8, the magnetic moment of bare surface Co atom is the same, 1.844 μB, which are mainly attributed to the unpaired d electrons. When CO adsorbs at the top site on Co(0001), the magnetic moment of Co atom directly bonding with CO greatly reduces by 0.799; while those of other atoms slightly increase. For CO adsorbed at the fcc or hcp hollow sites, the magnetic moments of the three Co atoms connected with CO reduce by 0.309~0.354 μB. Similar reduce are observed (about 0.45 μB) for the two Co atoms bonding with CO. The surface Co atoms without direct connection with CO remain almost unchanged. Similar results are also observed for the subsurface atoms

and are not listed herein. In summary, the electrons of surface Co bonding with CO transfer to the $2\pi^*$ orbitals, which directly leads to the reduction of magnetic moments of surface Co atoms. This is a directly theoretical evidence for the electronic donation from surface Co to CO.

Table 8 Magnetic moments and corresponding changes (µB) of surface cobalt atoms compared with the bare surface upon CO adsorption

slab	Magnetic moment				Magnetic moment change			
	top	fcc	hcp	bridge	top	fcc	hcp	bridge
Co1	1.84	1.89	1.88	1.50	1.87	0.04	0.04	-0.34	0.03
Co2	1.84	1.89	1.54	1.49	1.39	0.04	-0.31	-0.35	-0.46
Co3	1.84	1.05	1.52	1.49	1.84	-0.80	-0.33	-0.35	0.00
Co4	1.84	1.89	1.53	1.91	1.40	0.04	-0.32	0.06	-0.45

Note: Co1-Co4 atoms are labeled in Fig. S2 of supplementary material.

Here, we have to make a note. Although the reaction energy differences of FTS reactions in gas phase are better predicted by RPBE than by the other two functionals, it does not mean that this is true in any reactions. For other concerned reaction systems, the exchange-correlation functionals must be tested to find a proper one. On the other hand, B3LYP might not always obtain the accurate theoretical reference data ΔE_0 for any reactions. To obtain a reliable ΔE_0, the corresponding theoretical functional and level should also be tested by comparing ΔH with available experimental data.

4. CONCLUSION

In summary, a scheme to choose a proper functional for theoretical catalysis on surface is shown in Fig. 1. For a given system, ΔE_0 of the total reactions in gas phase reactions should be firstly tested, which is very fast and informative for screening exchange-correlation functionals; then the geometrical and electronic properties of substrate should be compared with the corresponding experiment; finally, the adsorption behaviors of typical probe molecule on modeling catalysts might be characterized and compared. This work has general significance for choosing a reliable exchange-correlation functional in the computational catalysis on surface.
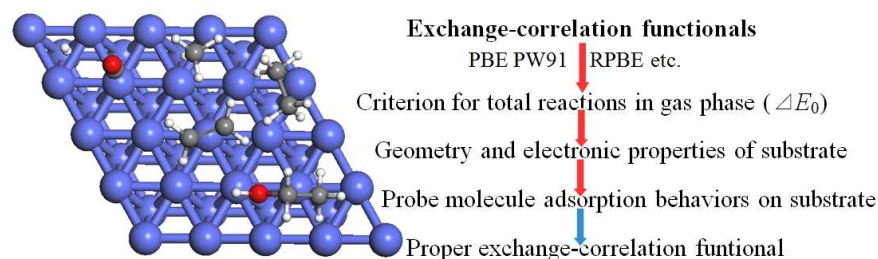

Fig. 2 A recommended scheme for choosing a proper exchange-correlation functional in theoretical catalysis on surface.

Notes and references

1. P. Geerlings, F. De Proft and W. Langenaeker, *Chem. Rev.*, 2003, **103**, 1793-1874.
2. A. J. Cohen, P. Mori-Sánchez and W. Yang, *Chem. Rev.*, 2011, **112**, 289-320.
3. B. Kaduk, T. Kowalczyk and T. Van Voorhis, *Chem. Rev.*, 2011, **112**, 321-370.
4. J. Hafner, *J. Comput. Chem.*, 2008, **29**, 2044-2078.
5. Y. S. Meng and M. E. Arroyo-de Dompablo, *Energy Environ. Sci.*, 2009, **2**, 589-609.
6. G. Rostamikia and M. J. Janik, *Energy Environ. Sci.*, 2010, **3**, 1262-1274.
7. H. Toulhoat, in *Encyclopedia of Materials: Science and Technology (Second Edition)*, eds. K. H. J. B. Editors-in-Chief: , W. C. Robert, C. F. Merton, I. Bernard, J. K. Edward, M. Subhash and V. Patrick, Elsevier, Oxford, Editon edn., 2010, pp. 1-7.
8. T. Bligaard, J. K. Nørskov and B. I. Lundqvist, in *Handbook of Surface Science*, eds. E. Hasselbrink and B. I. Lundqvist, North-Holland, Editon edn., 2008, vol. Volume 3, pp. 269-340.
9. J. K. Nørskov, T. Bligaard, J. Rossmeisl and C. H. Christensen, *Nature Chem.*, 2009, **1**, 37-46.
10. Y. Zhao, B.-T. Teng, X.-D. Wen, Y. Zhao, L.-H. Zhao and M.-F. Luo, *Catal. Commun.*, 2012, **27**, 63-68.
11. B.-T. Teng, F.-M. Wu, W.-X. Huang, X.-D. Wen, L.-H. Zhao and M.-F. Luo, *ChemPhysChem*, 2012, **13**, 1261-1271.
12. N. Martsinovich and A. Troisi, *Energy Environ. Sci.*, 2011, **4**, 4473-4495.
13. F. Li, S. Luo, Z. Sun, X. Bao and L.-S. Fan, *Energy Environ. Sci.*, 2011, **4**, 3661-3667.
14. I. Y. Zhang and X. Xu, *ChemPhysChem*, 2012, **13**, 1486-1494.
15. J. Paier, M. Marsman, K. Hummer, G. Kresse, I. C. Gerber and J. G. Angyan, *J. Chem. Phys.*, 2006, **124**, 154709.
16. A. Stroppa and G. Kresse, *New. J. Phys.*, 2008, **10**, 063020.
17. B. Hammer, L. B. Hansen and J. K. Nørskov, *Phys. Rev. B*, 1999, **59**, 7413-7421.

18. M. Gajdoš, A. Eichler and J. Hafner, *J. Phys. Condens. Mat.*, 2004, **16**, 1141.

19. M. Sierka, *Prog. Surf. Sci.*, 2010, **85**, 398-434.

20. D. R. Lide, ed., *CRC Handbook of Chemistry and Physics*, CRC Press, 2003-2004.

21. G. W. T. M. J. Frisch, H. B. Schlegel, G. E. Scuseria, M. A. Robb, J. R. Cheeseman, J. A. Montgomery, Jr., T. Vreven, K. N. Kudin, J. C. Burant, J. M. Millam, S. S. Iyengar, J. Tomasi, V. Barone, B. Mennucci, M. Cossi, G. Scalmani, N. Rega, G. A. Petersson, H. Nakatsuji, M. Hada, M. Ehara, K. Toyota, R. Fukuda, J. Hasegawa, M. Ishida, T. Nakajima, Y. Honda, O. Kitao, H. Nakai, M. Klene, X. Li, J. E. Knox, H. P. Hratchian, J. B. Cross, V. Bakken, C. Adamo, J. Jaramillo, R. Gomperts, R. E. Stratmann, O. Yazyev, A. J. Austin, R. Cammi, C. Pomelli, J. W. Ochterski, P. Y. Ayala, K. Morokuma, G. A. Voth, P. Salvador, J. J. Dannenberg, V. G. Zakrzewski, S. Dapprich, A. D. Daniels, M. C. Strain, O. Farkas, D. K. Malick, A. D. Rabuck, K. Raghavachari, J. B. Foresman, J. V. Ortiz, Q. Cui, A. G. Baboul, S. Clifford, J. Cioslowski, B. B. Stefanov, G. Liu, A. Liashenko, P. Piskorz, I. Komaromi, R. L. Martin, D. J. Fox, T. Keith, M. A. Al-Laham, C. Y. Peng, A. Nanayakkara, M. Challacombe, P. M. W. Gill, B. Johnson, W. Chen, M. W. Wong, C. Gonzalez, and J. A. Pople, *Gaussian, Inc., Wallingford CT*, 2004.

22. G. Kresse and J. Hafner, *Phys. Rev. B*, 1994, **49**, 14251.

23. J. A. White and D. M. Bird, *Phys. Rev. B*, 1994, **50**, 4954.

24. J. P. Perdew and Y. Wang, *Phys. Rev. B*, 1992, **45**, 13244-13249.

25. J. P. Perdew, K. Burke and M. Ernzerhof, *Physical Review Letters*, 1996, **77**, 3865-3868.

26. G. Kresse and D. Joubert, *Phys. Rev. B*, 1999, **59**, 1758.

27. H. J. Monkhorst and J. D. Pack, *Phys. Rev. B*, 1976, **13**, 5188.

28. B.-T. Teng, J.-J. Lang, X.-D. Wen, C. Zhang, M. Fan and H. G. Harris, *J. Phys. Chem. C*, 2013, **117**, 18986-18993.

29. M. D. Segall, P. J. D. Lindan, M. J. Probert, C. J. Pickard, P. J. Hasnip, S. J. Clark and M. C. Payne, *J. Phys. Condens. Mat.*, 2002, **14**, 2717.

30. J. Clark Stewart, D. Segall Matthew, J. Pickard Chris, J. Hasnip Phil, I. J. Probert Matt, K. Refson and C. Payne Mike, *Cryst. Mater.*, 2005, **220**, 567.

31. S. Baroni, S. de Gironcoli, A. Dal Corso and P. Giannozzi, *Rev. Mod. Phys.*, 2001, **73**, 515-562.

32. B. Montanari and N. M. Harrison, *Chem. Phys. Lett.*, 2002, **364**, 528-534.

33. R. B. Anderson, in *Stud. Surf. Sci. Catal.*, eds. S. Kaliaguine and A. Mahay, Elsevier, Editon edn., 1984, vol. Volume 19, pp. 457-461.

34. B.-T. Teng, C.-H. Zhang, J. Yang, D.-B. Cao, J. Chang, H.-W. Xiang and Y.-W. Li, *Fuel*, 2005, **84**, 791-800.

35. B.-T. Teng, J. Chang, C.-H. Zhang, D.-B. Cao, J. Yang, Y. Liu, X.-H. Guo, H.-W. Xiang and Y.-W. Li, *Appl. Catal. A*, 2006, **301**, 39-50.

36. M. Corral Valero and P. Raybaud, *Catal. Lett.*, 2013, **143**, 1-17.

37. R. A. Kendall, T. H. Dunning and R. J. Harrison, *J. Chem. Phys.*, 1992, **96**, 6796-6806.

38. D. Alfè, *Comput. Phys. Commun.*, 2009, **180**, 2622-2633.

39. H. Papp, *Surface Science*, 1983, **129**, 205-218.

40. G. A. Beitel, A. Laskov, H. Oosterbeek and E. W. Kuipers, *J. Phys. Chem.*, 1996, **100**, 12494-12502.

41. J. Lahtinen, J. Vaari, K. Kauraala, E. A. Soares and M. A. Van Hove, *Surf. Sci.*, 2000, **448**, 269-278.

42. J. J. C. Geerlings, M. C. Zonnevylle and C. P. M. de Groot, *Surf. Sci.*, 1991, **241**, 302-314.

43. D. Nabok, P. Puschnig and C. Ambrosch-Draxl, *Phys. Rev. B*, 2008, **77**, 245316.

44. B. M. Wong and S. H. Ye, *Phys. Rev. B*, 2011, **84**, 075115.